

STRUCTURAL IDENTIFICATION OF CUBIC ALUMINUM AND NON-CUBIC TITANIUM USING X-RAY DIFFRACTOMETER

¹D. Parajuli, ²G. C. Kaphle, ³N. Murali*, ⁴K. Samatha

¹Research Center for Applied Science and Technology, Tribhuvan University, Kirtipur, Kathmandu, Nepal

²Central Department of Physics, Tribhuvan University, Kirtipur, Kathmandu, Nepal.

³Department of Engineering Physics, Andhra University, Vishakhapatnam, India.

⁴Department of Physics, College of Science & Technology, Andhra University, Visakhapatnam, India

*Corresponding author email: muraliphdau@gmail.com

ABSTRACT

The unknown crystalline samples like minerals, inorganic compounds etc. are identified mostly with the help of X-ray diffraction (XRD). More than 25 Nobel prizes have been awarded to the works based on it. The identification of the solids are essential for the research in various streams of science like Material, Environmental, Geo, Engineering and Biology. The XRD is based on Bragg's law. The diffraction pattern obtained after passing the X-ray through interatomic slit is the main source of the structure. It was first demonstrated by Max von Laue (1912). The XRD is now attached with instrumental and computational tools. This paper focus on different steps for the indexing of an X-ray diffraction pattern, identifying the Bravais lattice, and calculating the lattice parameters of the cubic (Al) and non-cubic (Ti) system that are the starting elements we have used for the preparation of MXene. We have used the experimental and mathematical ways for the determinations of the intended structural values. The values obtained were in well agreement with the standard data.

Keywords: Crystalline samples, XRD, indexing, lattice parameters, cubic and non-cubic systems

I. INTRODUCTION

The structure of a material gives many of its important properties. It can be identified experimentally with X-ray diffractometer. It is a fast, simple and easy method to find the structural determination of thin films and bulk samples [1]. The results have high accuracy. We know that diffraction from an obstacle is possible only when the wavelength of the X-rays is in the order of the size of the obstacle. The interatomic distance of a crystal is in the same order with the wavelength of X-ray. In the X-rays diffraction, the X-rays are generated from the target with high atomic weight after being accelerated by high potential difference between the target and the filament. Here, both K_α and K_β are generated. The unnecessary k_β radiation can be removed using Ni-filter resulting a coherent and monochromatic X-ray beam. Bragg's law states that the diffraction takes place only when i) angle of incidence is equal to angle of scattering and ii) the path difference between the incident rays is integer multiple of the wavelength of X-ray used. In this condition, there is constructive interference between the rays in such a way that: $2d \sin(\theta) = n\lambda$, where d is the spacing between Bragg planes, θ is the incident angle, λ is the wavelength, and the integer n is the order of the scattered beam as shown in figure 1. The spacing between the Bragg planes " d " and inter-atomic distance " a " are related as: $a = d(h^2+k^2+l^2)^{1/2}$, where, the Miller indices (hkl) are defined as the reciprocals of the fractional intercepts. More than 25 scientists of different disciplines have achieved Nobel Prize using X-ray diffractometer. There are several methods of XRD. They are single crystal, fiber diffraction, powder diffraction (grinded specimen into powder to the size of about 10^{-4} cm) and Small Angle X-ray Scattering (nanoscale sample necessarily not crystal is detected within 0.1° - 10°) etc.

In the single crystal method, the crystal is mounted on a goniometer in order to align the crystal in desired direction. In this case, the diffraction pattern obtained are called reflections. The 2D images taken at different orientations can be converted into 3D with the help of Fourier Transform. Similar patterns can be obtained by electron or neutron diffraction for poor crystal. The single crystal method is rare. The scattering is elastic in all cases i.e. the wavelength of incoming and scattered wave is same. In the other hand, the inelastic method is used in the X-ray scattering involving the excitation of the samples like plasmons, crystal field, orbital excitations, phonons, magnons etc. rather than the distribution of its atoms [2].

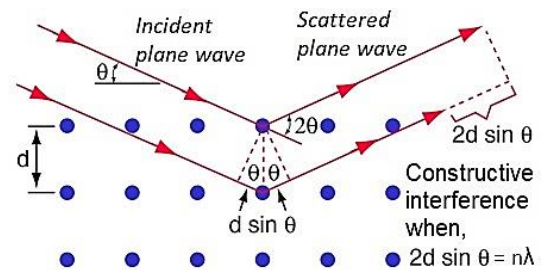


Fig 1: Bragg's Law

The amorphous has no order or specified structure. So, it is said to have short range order (SRO). These are characterized by broaden hump in low range of angles in XRD. The polycrystalline materials has some extent of order and called as medium range order (MRO). Few sharp peaks in specified direction can be seen in XRD. The intensity is higher than that in amorphous. The crystallite size can be calculated by Scherer formula [3-8]. The

single crystal materials has long range order (LRO). It has sharp diffraction peaks with preferred orientations in XRD. They have high intensity and low full width half maximum (FWHM). All parameters of crystal structure; lattice parameters, miller indices, particle size and micro-strain (in case of the presence of peak's shift) can be determined. The diffraction pattern for a piece of amorphous material (such as glass) usually appears as concentric rings around the un-scattered beam image. For crystal with regular spacing between atoms, the ring breaks up into spots. We have used this techniques for the structural characterization of several advanced materials [9–15].

II. MATERIALS AND METHODS

Sample Preparation, Selection of Single Crystal, Crystal Mounting, Determination of Unit Cell, Data Reduction, Space Group Determination, Electron Density, The Phase Problem, structure solution and direct method, Structure refinement, R factor determination, Crystallites size from Scherer's equation, Data Collection, Calculation and Indexing the Diffraction Patterns is done in this section. The material selected were two elements Aluminum in cubic and Titanium in non-cubic system. Their structural properties were studied with the help of X-Ray Diffractometer using $\text{CuK}\alpha$ radiation with wavelength $\lambda=540562 \text{ \AA}$ [16–23]. For the structural determination of cubic and non-cubic systems, there are mainly two ways: a) Mathematical and 2) Analytical. In mathematical, the smallest angle (corresponding to the first peak with high intensity) and in analytical the lowest common quotient is used for the calculation of the series which is tallied with the standard series to confirm the structure as described in the following sections.

III. EXPERIMENTAL STEPS AND THEORETICAL BACKGROUND

The experimental steps along with the theoretical background are discussed as follows:

A. Sample Preparation:

The material under study was prepared by the crystallization process. It is necessary to grow single crystals with edges around 0.10 to 0.30mm to perform X-ray crystallographic studies. The pure analytical grade Aluminum and Titanium were brought from the suppliers. Best crystals are usually produced when the solution is free from mechanical vibration and are allowed to evaporate without disturbance [24].

B. Selection of Single Crystal

The sample for identifying the structure should be a single crystal. It can be oriented randomly in any direction in the path of the X-ray beam in order to scatter and give a clear diffraction pattern. The good 3D X-ray diffraction data collection requires a single crystals free of defects such as twinning, voids, cracks etc. They can be examined under a polarizing microscope and select their best portion.

C. Shaping a Crystal

Nearly equi-dimensional crystal can be shaped by trimming irregular crystal. Trimming distort the edges of the crystal. This can be avoided by dressing for the Soft crystals. While hard crystals are

trimmed along certain planes. While cutting the crystal, its size should not be greater than the diameter of the collimator of XRD so that the crystal lies in the region of in X-ray beam at any orientation.

D. Crystal Mounting

The crystal is glued on a fiber glass and inserted into a goniometer head through a brass bin, which holds crystals in place on a diffractometer and can be moved linearly or circularly.

E. Determination of Unit Cell

The orientation of the crystal is recorded by a detector the quantum version of which scan the intensity of the reflected beam. The least square fitting of the shortest vector gives the intensity with the help of beam reflected from the reciprocal lattice. The three different crystallographic zones gives the 36 frames with the use of vector differences.

F. Data Reduction

The values of XRD are expressed in the terms of Miller indices incorporated with structure factor. The Lorentz (L) and polarization (p) factors should also be corrected [25].

G. Space Group Determination

If the lattice is not primitive, certain classes of hkl peaks will be missing and termed as systematic absences. These absences helps to determine the space group (or at least narrow down the possibilities). We know, there are 14 Bravais lattices. Their inversion, reflection, rotation and rotation-reflection symmetry give 32 point groups. Similarly, their screw and glide symmetry gives 230 space groups. Space group is a set of symmetry elements (on which symmetry operation is done) which completely describes the spatial arrangement of a 3D periodic pattern.

The nomenclature of space group has four parts: 1st is Bravais type and symmetry elements with respect to 3 given viewing directions as generators (i. e. 2nd is glide plane $c \perp a$, glide plane $a \perp b$, and screw axis lc). The Crystallographic Viewing directions are as in the table:

Crystal system	Viewing directions		
Triclinic	...		
Monoclinic	b (c)		
Orthorhombic	A	B	c
Tetragonal	C	a=b	[110]
Trigonal	C	a=b	[210]
Hexagonal	C	a=b	[210]
Cubic	a=b=c	[111]	[110]

In triclinic, there is no such specific viewing direction. There can be maximum of center of inversion which has no direction. In monoclinic symmetry element can be specified in one direction which is chosen by convention. International direction is b but c is preferred in some Eastern European countries. For tetragonal, trigonal, hexagonal, the rotational axis of highest order parallel of

the c-axis and respective direction as shown in table are the viewing directions. The glide planes and Screw Axes in the crystals [26] are discussed in supplementary information.

H. Structure Factor

The aggregate impact of j waves in hkl reflecting planes give the structure factor, F_{hkl} and depends on the scattering factor, f_j and phase δ of the atom in a unit cell. The maximum diffraction in terms of f_j and δ is called as structure factor and is obtained by $F_{hkl} = \sum_{j=1}^N \exp[2\pi i(hx_j + ky_j + lz_j)]$ in general, where, f_j is the atomic scattering factor for the j^{th} atom, x_j , y_j , z_j are the fractional coordinates of the j^{th} atom and N denotes the total number of atoms in the unit cell. Also, F_{hkl} is a complex quantity, written as $F_{hkl} = |F_{hkl}|e^{i\phi_{hkl}}$, $|F_{hkl}|$ and ϕ_{hkl} are structural amplitude and the phase angle of hkl reflecting plane.

I. Electron Density

The electron density in a crystal is given by, $\rho(x, y, z) = \frac{1}{V} \sum_h \sum_k \sum_l F_{hkl} \exp[-2\pi i(hx + ky + lz)]$ which is obtained by Fourier methods at different locations of a unit cell [27].

J. The Phase Problem, direct method and structure solution

Since, the diffraction intensities are proportional to structural factor ($\sqrt{I_{hkl}} \propto |F_{hkl}|$), $|F_{hkl}|$ are obtained easily determined but there is no information about the phase. This is called *phase problem*. This is mainly due to 1) the high energy of the X-ray (10^{18} Hz) by not detecting the electric field change in 10^{-18} sec 2) The reference to sample wave distance fluctuating from 10^{-11} m 3) There are no well-defined phase relationships between the incident waves and hence the diffracted wave. The phase problem is solved mainly by direct method, heavy atom methods, anomalous dispersion methods and isomorphous replacement methods for locating the approximate positions of all the atoms in a unit cell. This is called *structure solution*.

The direct method is used for light atoms and assumes that the electron density is positive everywhere (positivity) and the atoms are spherically symmetric (atomicity). The structure amplitudes and phases are linked to electron density by Fourier transformation *refinement*

The SHELX97 program package is used for the refinement of the data obtained. The program was forwarded by Professor George Sheldrick of University of Gottingen, Germany [28] to get the accurate atomic positions.

K. R factor

It is the degree of similarity between the calculated and observed diffraction pattern denoted by $|F_c|$ and $|F_o|$ respectively and given by $R = \frac{\sum |F_o| - |F_c|}{\sum |F_o|}$. In the same way, the weighted R-factor and goodness of fit can be done for more confirmation.

L. Crystallites size from Scherer's equation

The Scherer's Formula is, $D = \frac{k\lambda}{\beta \cos\theta}$ where, D = crystallites size (nm) for $k = 0.9$ (Scherer's constant), $\lambda = 0.15406$ nm (wavelength of the x-ray sources), β = FWHM (radians) and θ =

Peak position (radians). The peak position and FWHM are determined from XRD data [13,29–36].

IV. RESULT AND DISCUSSION

The Bravais lattice of a material is found in XRD JCPDS Card or other similar softwares. In the XRD pattern of a crystal; a) *relative positions* of the diffraction peaks gives the *shape and size* of the unit cell b) *relative intensities* of the diffraction peaks gives the *atomic position* within the unit cell. So, the unknown structure of a crystal can be determined mainly in three steps: 1) finding the shape and size of the crystal using angular position of the diffraction lines 2) the number of atoms per unit cell from shape and size, and 3) the position of the atom within the unit cell using the relative intensities of the diffraction lines.

Indexing the Diffraction Patterns

The process of determining the unit cell parameters from the peak positions with the help of miller indices is called indexing. For indexing diffraction pattern, each and every peak should be assigned by correct Miller indices as shown in figure 1 (Supplementary part). In cubic system, the indexing is done with three miller indices: h , k and l . But in non-cubic basically in hexagonal crystal, the indexing is done with four indices: h , k , i , and l (*three a_1 , a_2 , a_3 in basal and c as usual in perpendicular direction*). The three index system with respective unit vectors (UVW) can be transformed to four index system (uvw) with the following rule: $U = u - t$, $V = v - t$, $w = w$ and $u = 1/3(2U - V)$, $v = 1/3(2V - U)$, $t = -(u + v)$, $w = W$. In this indexing section of this paper, we will consider only three indices in all cases.

A. Indexing Cubic crystals

There are two methods of analysis for Indexing XRD pattern of the cubic material of ceramic, a semiconductor, a zeolite etc. (Here, we have taken aluminum. The XRD pattern for Aluminum is as shown in figure 2 in supplementary information.): a) Mathematical method and b) Analytical method.

1. Mathematical method

The Bragg's law gives the location of the peak with the help of miller indices hkl . θ_{hkl} is related to the interplanar spacing, d , as: $\lambda = 2d_{hkl} \sin \theta_{hkl}$, $1/d = 2 \sin \theta / \lambda$, $1/d^2 = 4 \sin^2 \theta / \lambda^2$. Or $\sin^2 \theta = \lambda^2 / 4d^2$. We know that, for a cubic phase the d -values can be calculated from the Miller indices (hkl): $1/d^2 = (h^2 + k^2 + l^2) / a^2$. Combining these two equations, we get the following relationship,

$$(h^2 + k^2 + l^2) / a^2 = 4 \sin^2 \theta / \lambda^2,$$

$$\text{Or, } \sin^2 \theta = (\lambda^2 / 4a^2) (h^2 + k^2 + l^2),$$

where, λ and a are constants, hence $\lambda^2 / 4a^2$ is constant for any pattern. "*Sin²θ is proportional to $h^2 + k^2 + l^2$ i.e., planes with higher Miller indices will diffract at higher values of θ.*" Then, for any two different planes, we get, $\frac{\sin^2 \theta_2}{\sin^2 \theta_1} = \frac{h_2^2 + k_2^2 + l_2^2}{h_1^2 + k_1^2 + l_1^2} * h, k, l$, are always integers.

In cubic system, the first XRD peak in the diffraction pattern (i.e. lower angle) will be due to diffraction from planes with the lowest Miller indices. For

- simple cubic, (100), $h^2 + k^2 + l^2 = 1$

- body-centered cubic, (110), $h^2 + k^2 + l^2 = 2$
- face-centered, (111), $h^2 + k^2 + l^2 = 3$

In the above expression*, $\theta_1 = \theta_{\min}$ and $h_1^2 + k_1^2 + l_1^2$ are the lowest Miller indices that corresponds to the minimum XRD peak in the pattern. The indices series for the respective Bravais lattices are listed in the table 1 (supplementary information). Comparing the series with the standard one, the Bravais lattice belongs to Face-Centered Cubic. The average lattice parameter 'a' from the table is 4.0539 Å.

Table 1: Allowed reflection for cubic lattices

Structure	Allowed Values	$h^2+k^2+l^2$
Primitive (Simple)	All possible h, k and l values	1, 2, 3, 4, 5, 6, 8, 9, 10...
Body-centered	(h + k + l) is even.	2, 4, 6, 8, 10, 12, 14, 16, ...
Face-centered	h, k and l are either all even or all odd but not mixed (odd even)	3, 4, 8, 11, 12, 16, 19, 20, 24, 27, 32...

Then, the ratio $(\sin^2\theta / \sin^2\theta_{\min})$ multiplied with 1, 2 and 3 corresponds to Simple cubic, body centered and face centered respectively. The series of values of $h_1^2 + k_1^2 + l_1^2$ obtained are compared with the series in the table 1. The tally one gives the Bravais lattice. Finally, the lattice parameter is obtained with the help of $(h^2 + k^2 + l^2) / a^2 = 4\sin^2\theta / \lambda^2$. Its average value is 4.0539 Å.

2. Analytical Method for cubic system (Aluminum):

In this method, the lowest common quotient (LCQ) is determined first and divide $\sin^2\theta$. The consequence obtained is tallied with the allowed reflection pattern for cubic lattices as mentioned in the table 2 (supplementary information).

B. Indexing for non-cubic structures (Titanium)

The XRD pattern of two samples of non-cubic Titanium atom are as shown in figure 3 and 4 (supplementary information). In case of system with lower symmetry, we need the information about the resulting lattice parameter ratios like c/a, b/a, etc. The plane spacing equations for some of the structures including Bragg's law are as:

$$\text{Hexagonal } \frac{1}{d^2} = \frac{4}{3} \frac{h^2 + hk + k^2}{a^2} + \frac{l^2}{c^2} = \frac{4\sin^2\theta}{\lambda^2}$$

$$\sin^2\theta = \frac{\lambda^2}{4} \left(\frac{4}{3} \frac{h^2 + hk + k^2}{a^2} + \frac{l^2}{c^2} \right)$$

$$\text{Tetragonal } \frac{1}{d^2} = \frac{h^2 + k^2}{a^2} + \frac{l^2}{c^2} = \frac{4\sin^2\theta}{\lambda^2}$$

$$\sin^2\theta = \frac{\lambda^2}{4} \left(\frac{h^2 + k^2}{a^2} + \frac{l^2}{c^2} \right)$$

$$\text{Orthorhombic } \frac{1}{d^2} = \frac{h^2}{a^2} + \frac{k^2}{b^2} + \frac{l^2}{c^2} = \frac{4\sin^2\theta}{\lambda^2} \text{ etc.}$$

$$\sin^2\theta = \frac{\lambda^2}{4} \left(\frac{h^2}{a^2} + \frac{k^2}{b^2} + \frac{l^2}{c^2} \right)$$

Unlike cubic system having $\lambda^2/4a^2$ constant, our result here depends on the ratios of the lattice parameter like c/a, b/a, b/c etc. which is due to non-equivalence of indices in these system like tetragonal: 001≠100; orthorhombic: 001≠010≠100 etc... Similar to the cubic system, Indexing of non-cubic system can also be done by

- Mathematical Analysis
- Analytical Analysis
- Graphical or Dull and Davey Analysis [29]. Graphical method is not discussed here.

1. Mathematical method for non-cubic system

At first, the peaks in the XRD pattern are identified. We have,

$$\sin^2\theta = \left(\frac{\lambda^2}{4a^2} \right) \left(\frac{4}{3} (h^2 + hk + k^2) + \frac{l^2}{(c/a)^2} \right)$$

Here, the lattice parameter 'a' and the ratio of lattice parameters c/a are constant for a given diffraction pattern. Thus, $\frac{\lambda^2}{4a^2}$ is constant for any pattern. The value of 1st term, $\frac{4}{3} (h^2 + hk + k^2)$ depends on the other indices h and k as in the table 2.

 TABLE 2: Value of 1st term for various h and k

1 st term	K				
	0	1	2	3	4
h	1	0.000	1.333	5.333	12.000
	2	1.333	4.000	9.333	17.333
	3	5.333	9.333	16.000	25.333
	4	12.000	17.333	25.333	36.000

The second term $\frac{l^2}{(c/a)^2}$ can be determined by substituting the known c/a ratio. e. g. For zinc c/a=1.8563

 TABLE 3: Value of 2nd term for different l

l	l ²	l ² /(c/a) ²
0	0	0.000
1	1	0.290
2	4	1.161
3	9	2.612
4	16	4.643
5	25	7.255
6	36	10.447

Now, we have to add the allowed hkl valued of the two terms (the structure factor rule) and ranking in increasing order. The structure factor give rise to the following rules for hexagonal systems: 1) When $h + 2k = 3N$ (where N is an integer), there is no peak. 2) When l is odd, there is no peak. These both should be satisfied.

TABLE 4: Allowed and restricted values of hkl

Indices (hkl)	<i>l</i>	h+2k	Peak
301	Odd	3	No
103	Odd	1≠3N	Yes
etc.

We can assign the values in the same sequence for respective peaks in a hexagonal. Lattice parameters (a, b, c) can be determined in two steps:

1) We can find the value of ‘a’ (=b for hexagonal) by looking (hk0) planes i.e. $l=0$, for which the equation becomes, $\sin^2\theta = \left(\frac{\lambda^2}{4a^2}\right)\left(\frac{4}{3}(h^2 + hk + k^2)\right)$

$$a = \left(\frac{\lambda}{\sqrt{3} \sin\theta}\right) \sqrt{h^2 + hk + k^2}$$

We can find the value of ‘a’ for every (hk0) planes, the average of which gives final ‘a’.

2) For $h=k=0$, $c = \frac{\lambda}{2\sin\theta}l$. It gives the values of ‘c’ for every (00l) planes. Their average gives final ‘c’.

The values obtained from 1) and 2) are added and arranged in an increasing order which works as indices to the peaks of the diffraction pattern obtained especially for the powder XRD. The hk0 type of reflections were viewed and calculated ‘a’ for these reflections. 00l type reflections were viewed and calculated the ‘c’ for these reflections.

2. Analytical method for non-cubic Crystals (Ti)

$$\text{We have, } \sin^2\theta = \left(\frac{\lambda^2}{4a^2}\right)\left(\frac{4}{3}(h^2 + hk + k^2) + \frac{l^2}{(c/a)^2}\right)$$

$$\text{Or, } \sin^2\theta = A(h^2 + hk + k^2) + Cl^2$$

Where, $A = \frac{\lambda^2}{3a^2}$ and $C = \frac{\lambda^2}{4c^2}$ since, h, k, and l are always integers, the term $h^2 + hk + k^2$ can only have the values like 0, 1, 3, 7, 9, 12... and l^2 can only have values like 0, 1, 4, 9...

In this method, the peaks are identified and $\sin^2\theta$ for each peak are calculated, each $\sin^2\theta$ are divided by the integers 3, 4, 7, 9.... Lowest common coefficient is identified say A. The hk0 type indices are assigned to peaks, $\sin^2\theta - nA$ where $n = 1, 3, 4, 7, \dots$ are calculated. The lowest common quotient is found to identify 00l type peaks. For hexagonal system, 001 is forbidden and 002 will be the first peak for 00l. $Cl^2 = \sin^2\theta - A(h^2 + hk + k^2)$ gives the value of C. Look for values of $\sin^2\theta$ that increase by factors of 4, 9... which are the square terms for $l = 1, 2, 3, \dots$ and can be expressed as 004, 009,.... The values of A and C cannot give the values of hk0 and 00l. The lattice parameters are calculated from the values of A and Cas shown in table 6 (supplementary information). The lattice parameters a, c and their ratio c/a of non-cubic Titanium is found to be 2.951au, 4.686 au and 1.588au respectively. The detailed calculations are given in the table 3, 4, 5, 6 on supplementary information for two samples of Titanium.

V. CONCLUSIONS

The theoretical background, experimental approach and different calculation methods for finding the structural parameters

and indexing the XRD pattern were studied which gives the lattice parameters, symmetry group, space group and positions of the atoms in the unit cell. The indexing of cubic (Al) and non-cubic (Ti) system with different methods were in well agreement with the standard data which indicate the reliability of the method used. The average lattice parameter ‘a’ for cubic Aluminum The average lattice parameter of Aluminum by analytical and mathematical methods are 4.0539 Å and 4.0541 Å respectively. The lattice parameters a, c and their ratio c/a of non-cubic Titanium is found to be 2.951au, 4.686 au and 1.588au respectively and are in well agreement with International Center for Diffraction Data (ICDD) value 1.5871au.

References

- [1] R. Meshkian, *Synthesis and Characterization of Mo-and W-Based Atomic Laminates* (1933).
- [2] J. Fink, E. Schierle, E. Weschke, and J. Geck, *Resonant Elastic Soft X-Ray Scattering*, Reports Prog. Phys. **76**, (2013).
- [3] C. Komali, N. Murali, D. Parajuli, A. Ramakrishna, Y. Ramakrishna, and K. Chandramouli, *Effect of Cu2+ Substitution on Structure, Morphology, and Magnetic Properties of Mg-Zn Spinel Ferrite*, Indian J. Sci. Technol. **14**, 2309 (2021).
- [4] K. Subrahmanya Sarma, C. Rambabu, G. Vishnu Priya, M. K. Raju, D. Parajuli, B. Khalid Mujasam, V. Ritesh, K. Rajesh, N. Murali, and P. V. Lakshminarayana, *Enhanced Structural and Magnetic Properties of Al-Cr-Substituted SrFe12O19 Hexaferrite System*, Appl. Phys. A Mater. Sci. Process. **128**, 1 (2022).
- [5] S. Ravi Kumar, G. Vishnu Priya, B. Aruna, M. K. Raju, D. Parajuli, N. Murali, R. Verma, K. Mujasam Batoo, R. Kumar, and P. V. Lakshmi Narayana, *Influence of Nd3+ Substituted Co0.5Ni0.5Fe2O4 Ferrite on Structural, Morphological, Dc Electrical Resistivity and Magnetic Properties*, Inorg. Chem. Commun. **136**, 109132 (2022).
- [6] G. V. Priya, S. R. Kumar, B. Aruna, M. K. Raju, D. Parajuli, N. Murali, and P. V. L. Narayana, *Effect of Al 3+ Substitution on Structural and Magnetic Properties of NiZnCo Nano Ferrites*, (2021).
- [7] K. Ramanjaneyulu, B. Suryanarayana, V. Raghavendra, N. Murali, D. Parajuli, and K. Chandramouli, *Synthesis, Microstructural and Magnetic Properties of Cu Doped Mg0.5Zn0.5Fe2O4 Ferrites*, Solid State Technol. **64**, 7192 (2021).
- [8] G. K. Williamson and W. H. Hall, *X-Ray Line Broadening from Filled Aluminium and Wolfram*, Acta Metall. **1**, 22 (1953).
- [9] D. Parajuli and K. Samatha, *Structural Analysis of Cu Substituted Ni/Zn in Ni-Zn Ferrite*, BIBECHANA **18**, 128 (2021).
- [10] D. Parajuli and K. Samatha, *Morphological Analysis of Cu Substituted Ni/Zn in Ni-Zn Ferrites*, BIBECHANA **18**, 80 (2021).
- [11] D. Parajuli, N. Murali, and K. Samatha, *Correlation between the Magnetic and DC Resistivity Studies of Cu Substituted Ni and Zn in Ni-Zn Ferrites*, BIBECHANA **19**, 61 (2022).
- [12] D. Parajuli, V. Raghavendra, B. Suryanarayana, P. A. Rao, N. Murali, P. V. S. K. P. Varma, R. G. Prasad, Y. Ramakrishna, and K. Chandramouli, *Corrigendum to “Cadmium Substitution Effect on Structural, Electrical and Magnetic Properties of Ni-Zn Nano Ferrites” [Results Phys. 19 (2020) 2211-379 103487]*, Results Phys. **23**, 103947 (2021).

- [13] D. Parajuli, V. K. Vagolu, K. Chandramoli, N. Murali, and K. Samatha, *Electrical Properties of Cobalt Substituted NZCF and ZNCF Nanoparticles Prepared by the Soft Synthesis Method*, J. Nepal Phys. Soc. **8**, 45 (2022).
- [14] D. Parajuli, V. K. Vagolu, K. Chandramoli, N. Murali, and K. Samatha, *Soft Chemical Synthesis of Nickel-Zinc-Cobalt-Ferrite Nanoparticles and Their Structural, Morphological and Magnetic Study at Room Temperature*, J. Nepal Phys. Soc. **7**, 14 (2021).
- [15] D. Parajuli, N. Murali, and K. Samatha, *Structural, Morphological, and Magnetic Properties of Nickel Substituted Cobalt Zinc Nanoferrites at Different Sintering Temperature*, J. Nepal Phys. Soc. **7**, 24 (2021).
- [16] U. R. Gudla, B. Suryanarayana, V. Raghavendra, K. A. Emmanuel, N. Murali, P. Tadesse, D. Parajuli, K. Chandra Babu Naidu, Y. Ramakrishna, and K. Chandramouli, *Optical and Luminescence Properties of Pure, Iron-Doped, and Glucose Capped ZnO Nanoparticles*, Results Phys. **19**, 103508 (2020).
- [17] U. R. Gudla, B. Suryanarayana, V. Raghavendra, D. Parajuli, N. Murali, S. Dominic, Y. Ramakrishna, and K. Chandramouli, *Structural, Optical and Luminescence Properties of Pure, Fe-Doped and Glucose-Capped CdO Semiconductor Nanoparticles for Their Antibacterial Activity*, J. Mater. Sci. Mater. Electron. **32**, 3920 (2021).
- [18] K. Chandramouli, B. Suryanarayana, T. A. Babu, V. Raghavendra, D. Parajuli, N. Murali, V. Malapati, T. W. Mammo, P. S. V. Shanmukhi, and U. R. Gudla, *Synthesis, Structural and Antibacterial Activity of Pure, Fe Doped, and Glucose Capped ZnO Nanoparticles*, Surfaces and Interfaces **26**, 101327 (2021).
- [19] P. Himakar, K. Jayadev, D. Parajuli, N. Murali, P. Tadesse, S. Y. Mulushoa, T. W. Mammo, B. Kishore Babu, V. Veeraiah, and K. Samatha, *Effect of Cu Substitution on the Structural, Magnetic, and Dc Electrical Resistivity Response of Co_{0.5}Mg_{0.5}-XCu_xFe₂O₄ Nanoferrites*, Appl. Phys. A Mater. Sci. Process. **127**, 1 (2021).
- [20] P. Himakar, N. Murali, D. Parajuli, V. Veeraiah, K. Samatha, T. W. Mammo, K. M. Bato, M. Hadi, E. H. Raslan, and S. F. Adil, *Magnetic and DC Electrical Properties of Cu Doped Co-Zn Nanoferrites*, J. Electron. Mater. **50**, 3249 (2021).
- [21] K. Chandramouli, B. Suryanarayana, P. V. S. K. Phanidhar Varma, V. Raghavendra, K. A. Emmanuel, P. Tadesse, N. Murali, T. Wegayehu Mammo, and D. Parajuli, *Effect of Cr³⁺ Substitution on Dc Electrical Resistivity and Magnetic Properties of Cu_{0.7}Co_{0.3}Fe_{2-x}Cr_xO₄ Ferrite Nanoparticles Prepared by Sol-Gel Auto Combustion Method*, Results Phys. **24**, 104117 (2021).
- [22] K. C. P. V. S. K. Phanidhar Varma, B. Suryanarayana, Vemuri Raghavendra, D. Parajuli, N. Murali, *Effect of Cr Substitution on Magnetic Properties of Co-Cu Nano Ferrites.*, Solid State Technol. **63**, 8820 (2020).
- [23] A. M. Sankpal, S. V. Kakatkar, N. D. Chaudhari, R. S. Patil, S. R. Sawant, and S. S. Suryavanshi, *Initial Permeability Studies on Al³⁺ and Cr³⁺ Substituted Ni-Zn Ferrites*, J. Mater. Sci. Mater. Electron. **9**, 173 (1998).
- [24] H. Fieß, G. H. Stout, L. H. Jensen: *X-Ray Structure Determination, A Practical Guide, Second Edition*, John Wiley & Sons, New York, Chichester 1989. ISBN 0-471-60711-8, 453 Seiten, Preis: £ 75.50, Berichte Der Bunsengesellschaft Für Phys. Chemie **95**, 104 (1991).
- [25] Bruker (2004) *Advanced X-Ray Solutions. SAINT and SADABS Programs*. Bruker AXS Inc., Madison. - References - Scientific Research Publishing, <https://scirp.org/reference/referencespapers.aspx?referenceid=2384094>.
- [26] F. Hoffmann and M. Sartor, *The Fascination of Crystals and Symmetry Unit 4.6*, (n.d.).
- [27] H. Li, M. He, and Z. Zhang, *Evaluating the Electron Density Model by Applying an Imaginary Modification*, Powder Diffr. **33**, 4 (2017).
- [28] G. M. Sheldrick, *A Short History of SHELX*, Acta Crystallogr. Sect. A Found. Crystallogr. **64**, 112 (2008).
- [29] B. Cullity, *Elements of X-Ray Diffraction* (Addison-Wesley Pub. Co., Reading Mass., 1956).
- [30] H. R. Daruvuri, N. Murali, M. Madhu, A. Ramakrishna, D. Parajuli, and M. P. Dasari, *Effects of Zn²⁺ Substitution on the Structural, Morphological, DC Electrical Resistivity, Permeability and Magnetic Properties of Co_{0.5}Cu_{0.5-x}Zn_xFe₂O₄ Nanoferrite*, Appl. Phys. A Mater. Sci. Process. **129**, 1 (2023).
- [31] D. Parajuli, S. Uppugalla, N. Murali, A. Ramakrishna, B. Suryanarayana, and K. Samatha, *Synthesis and Characterization MXene-Ferrite Nanocomposites and Its Application for Dying and Shielding*, Inorg. Chem. Commun. **148**, 110319 (2023).
- [32] D. Parajuli, N. Murali, K. Samatha, and V. Veeraiah, *Thermal, Structural, Morphological, Functional Group and First Cycle Charge/Discharge Study of Co Substituted LiNi_{1-x}-0.02Mg_{0.02}CoxO₂ (x = 0.00, 0.02, 0.04, 0.06, and 0.08) Cathode Material for LIBs*, AIP Adv. **12**, 085010 (2022).
- [33] D. Parajuli, N. Murali, A. V. Rao, A. Ramakrishna, Y. M. S, and K. Samatha, *Structural, Dc Electrical Resistivity and Magnetic Investigation of Mg, Ni, and Zn Substituted Co-Cu Nano Spinel Ferrites*, South African J. Chem. Eng. **42**, 106 (2022).
- [34] D. Parajuli, P. Tadesse, N. Murali, and K. Samatha, *Study of Structural, Electromagnetic and Dielectric Properties of Cadmium Substituted Ni-Zn Nanosized Ferrites*, J. Indian Chem. Soc. **99**, 100380 (2022).
- [35] D. Parajuli, P. Tadesse, N. Murali, and K. Samatha, *Correlation between the Structural, Magnetic, and Dc Resistivity Properties of Co_{0.5}Mg_{0.5}-XCu_xFe₂O₄ (M = Mg, and Zn) Nano Ferrites*, Appl. Phys. A Mater. Sci. Process. **128**, 1 (2022).
- [36] D. Parajuli, K. C. Devendra, T. G. Reda, G. M. Sravani, N. Murali, and K. Samatha, *RHEED Analysis of the Oxidized M²M^xY₂ene Sheets by Ablated Plasma Thrust Method in Pulsed Laser Deposition Chamber*, AIP Adv. **11**, 115019 (2021).

Supporting information (SI) Figures and Tables

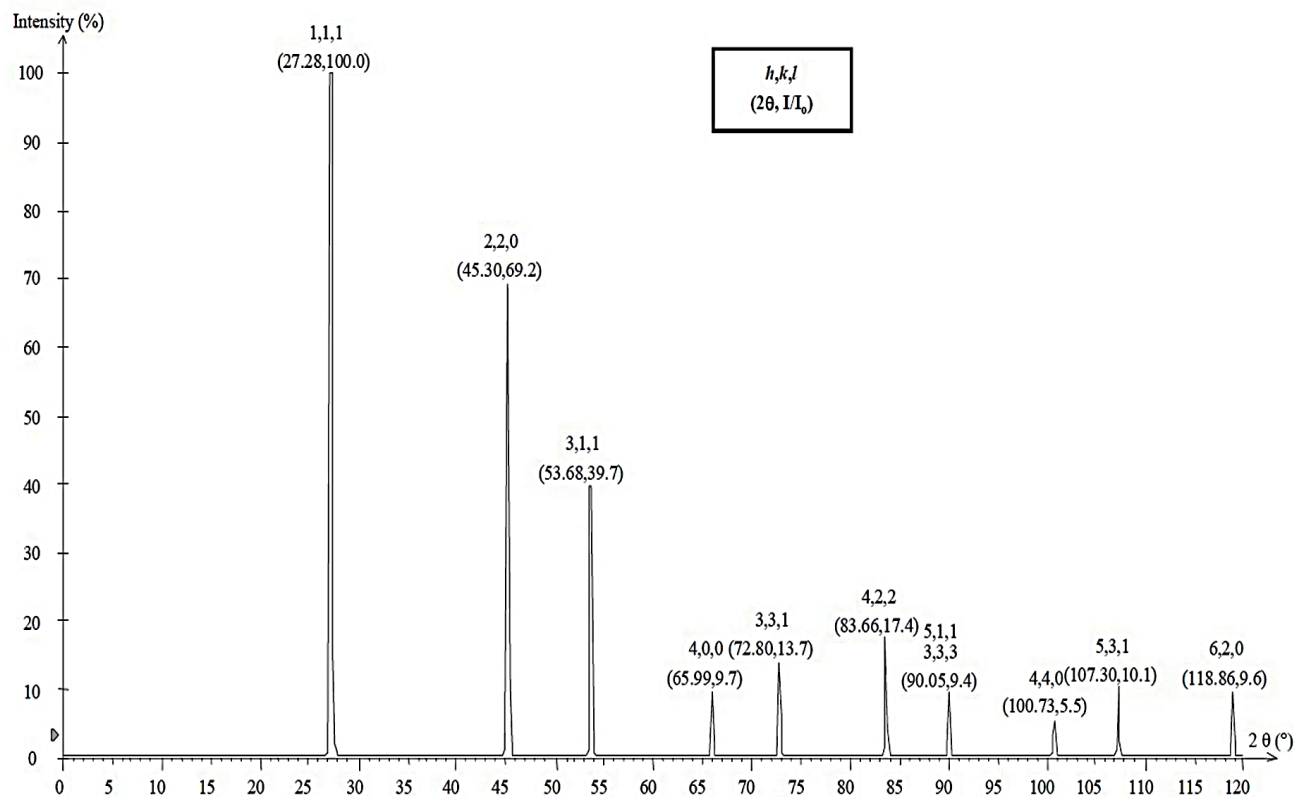


Fig 1: Diffraction pattern with proper indices

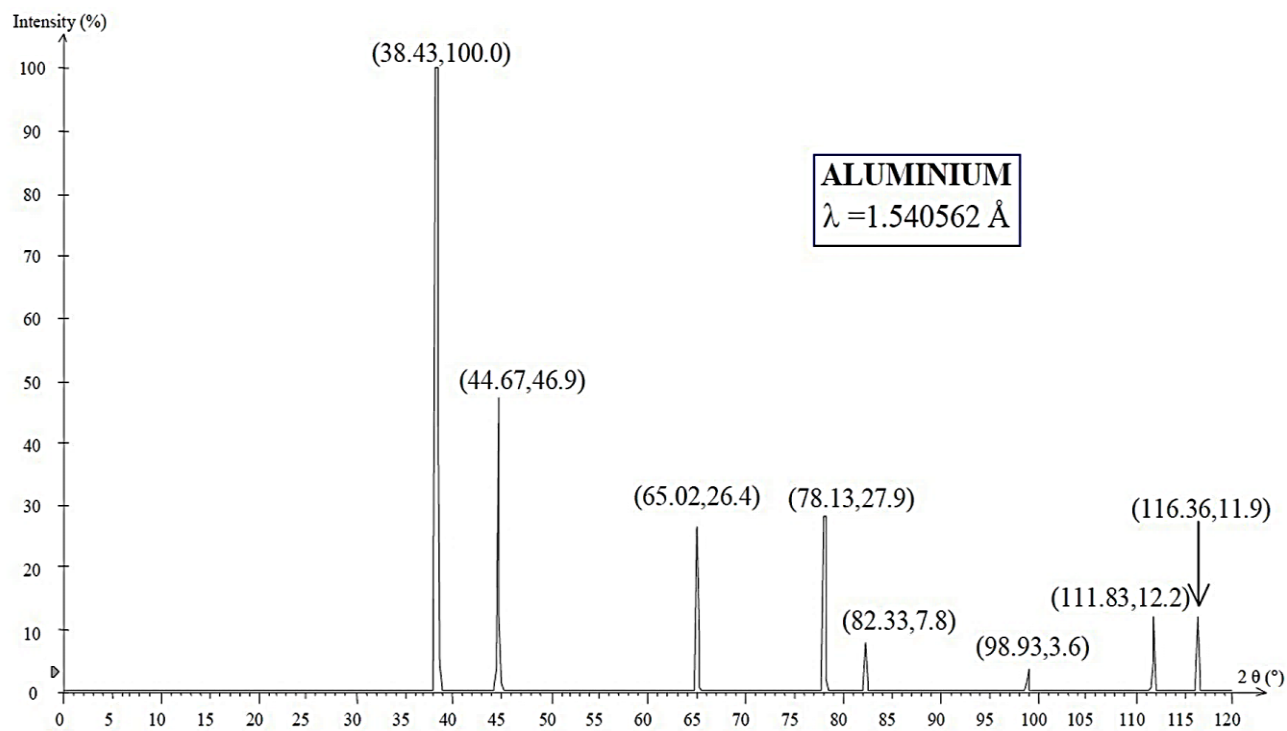


Fig 2: XRD pattern of Aluminum using CuKα radiation*

*Parameters related to maximum intensity are used for various calculation in Scherer's Formula.

Table 1: Calculation of lattice parameter of Aluminum unit cell by Mathematical Method.

Peak No.	$2\theta_2$	$\sin^2\theta_2$	$1 \times \frac{\sin^2\theta_2}{\sin^2\theta_{min}}$	$2 \times \frac{\sin^2\theta_2}{\sin^2\theta_{min}}$	$3 \times \frac{\sin^2\theta_2}{\sin^2\theta_{min}}$	$h_2^2 + k_2^2 + l_2^2$	Hkl	a (A°)
1	38.43	0.1083	1.000	2.000	3.000	3	111	4.0538
2	44.67	0.1444	1.333	2.667	4.000	4	200	4.0539
3	65.02	0.2888	2.667	5.333	8.000	8	220	4.0538
4	78.13	0.3972	3.667	7.333	11.000	11	311	4.0538
5	82.33	0.4333	4.000	8.000	12.000	12	222	4.0538
6	98.93	0.5776	5.333	10.665	15.998	16	400	4.0541
7	111.83	0.6859	6.333	12.665	18.998	19	331	4.0540
8	116.36	0.7220	6.666	13.331	19.997	20	420	4.0541

Comparing this series with the standard one (Table 1 in the main text), the Bravais lattice belongs to Face-Centered Cubic. The average lattice parameter 'a' from the table is 4.0539 A°.

Table 2: Calculation of lattice parameter of Aluminum unit cell by Analytical Method.

Peak No.	$2\theta_2$	$\frac{\sin^2\theta_2}{1}$	$\frac{\sin^2\theta_2}{2}$	$\frac{\sin^2\theta_2}{3}$	$\frac{\sin^2\theta_2}{4}$	$\frac{\sin^2\theta_2}{5}$	$\frac{\sin^2\theta_2}{6}$	$\frac{\sin^2\theta_2}{8}$	$\frac{\sin^2\theta_2}{K}$
1	38.43	0.1083	0.0542	0.0361	0.0271	0.0217	0.0181	0.0135	3.000
2	44.67	0.1444	0.0722	0.0481	0.0361	0.0289	0.0241	0.0181	4.000
3	65.02	0.2888	0.1444	0.0481	0.0722	0.0578	0.0481	0.0361	8.001
4	78.13	0.3972	0.1986	0.1324	0.0993	0.0794	0.0662	0.0496	11.001
5	82.33	0.4333	0.2166	0.1444	0.1083	0.0867	0.0722	0.0542	12.002
6	98.93	0.5776	0.2888	0.1925	0.1444	0.1155	0.0963	0.0722	16.000
7	111.83	0.6859	0.3430	0.2286	0.1715	0.1372	0.1143	0.0857	19.001
8	116.36	0.7220	0.3610	0.2407	0.1805	0.1444	0.1203	0.0903	20.000

*The lowest common quotient obtained from 5th, 6th, 9th column is K =0.0361. The sequence in the 10th column corresponds to Face Centered Cubic Bravais Lattice. Then, the lattice parameter is given by a= $\lambda/(2\sqrt{K})=4.0541$ A°. This method work for any cubical material like metal, ceramics, ionic crystals, minerals, intermetallics, semiconductors, etc.

Titanium Powder (-325 mesh)

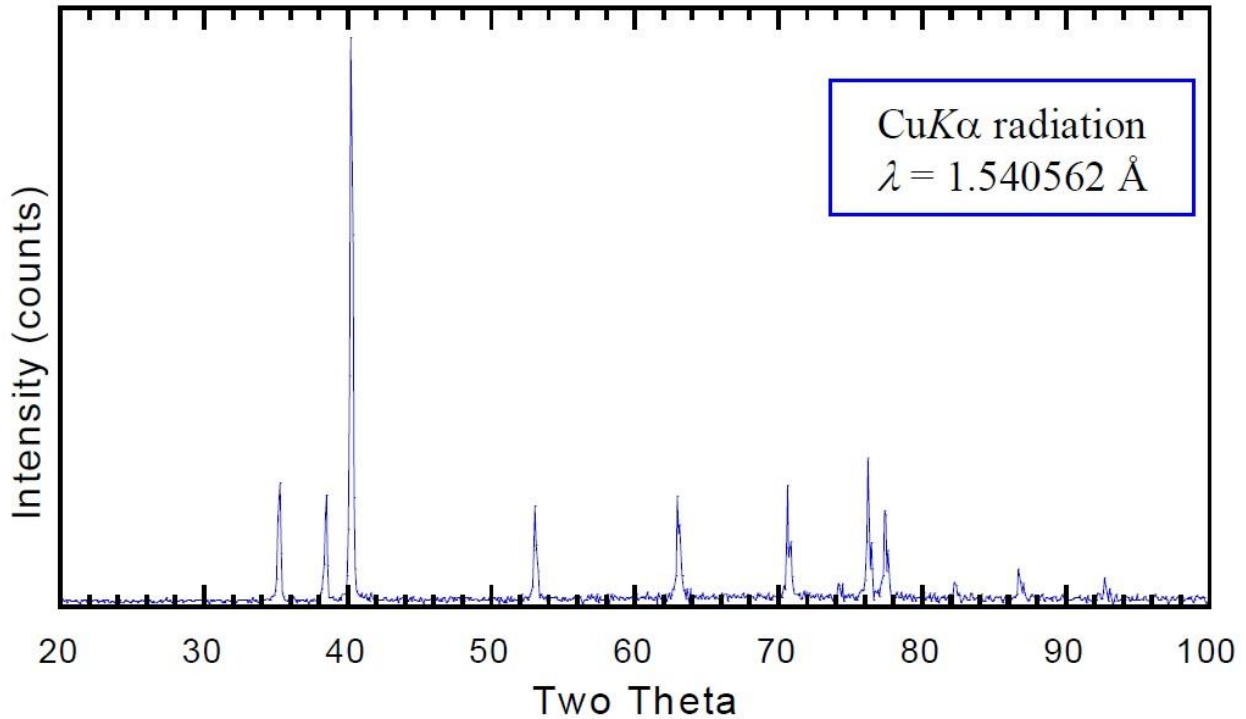


Fig 3: XRD pattern for the first sample of Titanium without indices

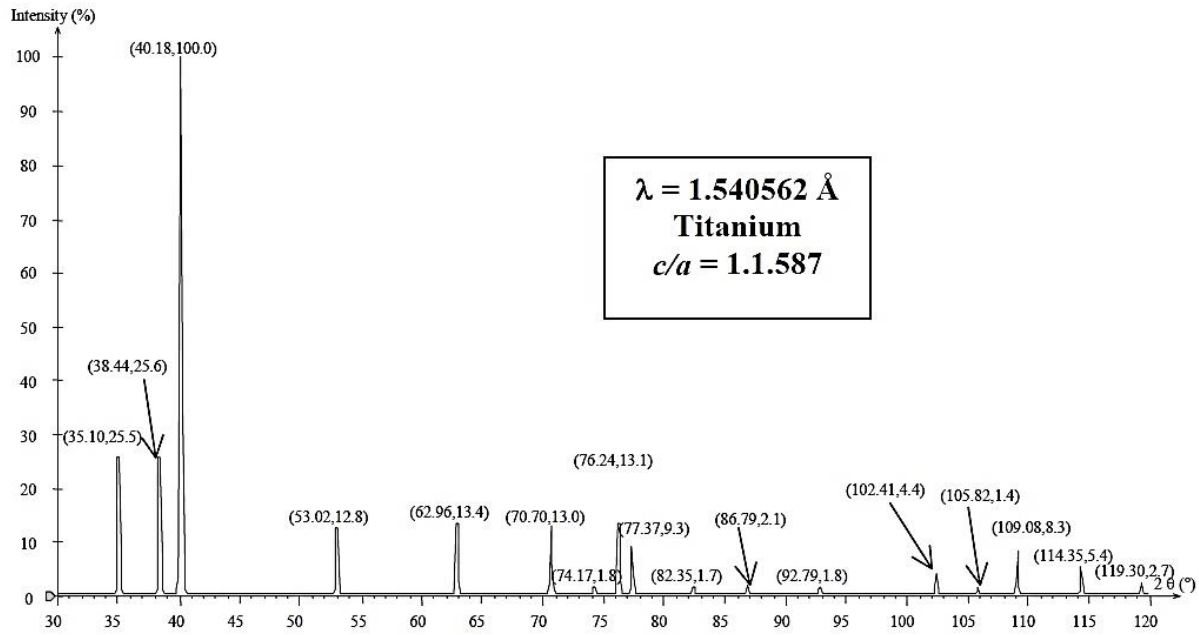


Fig 4: Diffraction pattern for another sample of Titanium

Table 3: Lattice parameter of Titanium (Sample 1) - a non-cubic Crystal by Mathematical method.

Peak(2θ)	Sin ² θ	d(nm)	hkl	h ² +hk+k ²	l ²	a (for l=0)	c (for h=k=0)
35.275	0.091805	2.5423	100	1	4	2.936	
38.545	0.108941	2.3338	002				4.668
40.320	0.118779	2.2351	101				
53.115	0.199895	1.7229	102				
63.095	0.273744	1.4723	110	3		2.945	
70.765	0.335278	1.3303	103				
74.250	0.36428	1.2763	200	4		2.947	
76.365	0.382132	1.2461	112				
77.500	0.39178	1.2307	201				
82.360	0.433526	1.1699	004		16		4.680
86.940	0.473309	1.1197	202				
92.900	0.525296	1.0628	104				
Average						2.943	4.674

The average value of c/a is found to be 1.588au and agrees with International Center for Diffraction Data (ICDD) value 1.5871.

The sample is changed for analytical method.

Table 4: Lattice parameter of Titanium (Sample 2) - a non-cubic crystal by Analytical method. (For l=0)

Peak (2θ)	I/I ₀	Sin ² θ	(Sin ² θ)/3	(Sin ² θ)/4	(Sin ² θ)/7	(Sin ² θ)/9	(Sin ² θ)/12	hkl	(Sin ² θ)/LCQ
35.100	25.5	0.0909	0.0303	0.0227	0.0130	0.0101	0.0076	100	1.0
38.390	25.6	0.1081	0.0360	0.0270	0.0154	0.0120	0.0090		1.2
40.170	100	0.1179	0.0393	0.0295	0.0168	0.0131	0.0098		1.3
53.000	12.8	0.1991	0.0664	0.0498	0.0284	0.0221	0.0166		2.2
62.940	13.4	0.2725	0.0908	0.0681	0.0389	0.0303	0.0227	110	3.0
70.650	13	0.3343	0.1114	0.0836	0.0478	0.0371	0.0279		3.7
74.170	1.8	0.3636	0.1212	0.0909	0.0519	0.0404	0.0303	200	4.0
76.210	13.1	0.3808	0.1269	0.0952	0.0544	0.0423	0.0317		4.2
77.350	9.3	0.3905	0.1302	0.0976	0.0558	0.0434	0.0325		4.3
82.200	1.7	0.4321	0.1440	0.1080	0.0617	0.0480	0.0360		4.8
86.740	2.1	0.4716	0.1572	0.1179	0.0674	0.0524	0.0393		5.2
92.680	1.8	0.5234	0.1745	0.1308	0.0748	0.0582	0.0436		5.8
102.350	4.4	0.6069	0.2023	0.1517	0.0867	0.0674	0.0506		6.7
105.600	1.4	0.6345	0.2115	0.1586	0.0906	0.0705	0.0529	210	7.0
109.050	8.3	0.6632	0.2211	0.1658	0.0947	0.0737	0.0553		7.3

114.220	5.4	0.7051	0.2350	0.1763	0.1007	0.0783	0.0588	7.8
119.280	2.7	0.7445	0.2482	0.1861	0.1064	0.0827	0.0620	8.2

Here, the lowest common quotient, **A=0.0908**. The allowed h^2+hk+k^2 value multiplied with LCQ corresponds with the respective value of $\sin^2\theta$. i.e. $3xA=0.27250$, $4xA=0.3636$, $7xA=0.6345$. The hkl values 9th column are the indices corresponding to: $h^2+hk+k^2 = 1, 3, 4, 7 \dots$ in the 10th column or $hk=10, 11, 20, 21$.

Table 5: Lattice parameter of Titanium sample 2- a non-cubic Crystal by Analytical method. (h=k=0)

Peak (2θ)	I/Io	Sin ² θ	Sin ² θ-A	Sin ² θ-3A	Sin ² θ-4A	Sin ² θ-7A	hkl	C=LCQ/I ²	I ² =LCQ/C
35.100	25.5	0.0909					100		
38.390	25.6	0.1081	0.0173				002	0.0270	4
40.170	100	0.1179	0.0271						
53.000	12.8	0.1991	0.1083				102	0.0271	
62.940	13.4	0.2725	0.1817	0.0001			110		
70.650	13	0.3343	0.2435	0.0618					
74.170	1.8	0.3636	0.2728	0.0911	0.0003		200		
76.210	13.1	0.3808	0.2900	0.1083	0.0175		112		
77.350	9.3	0.3905	0.2997	0.1180	0.0272				
82.200	1.7	0.4321	0.3413	0.1597	0.0688		004	0.0270	16
86.740	2.1	0.4716	0.3808	0.1991	0.1083		202	0.0271	
92.680	1.8	0.5234	0.4326	0.2509	0.1601				
102.350	4.4	0.6069	0.5161	0.3345	0.2436				
105.600	1.4	0.6345	0.5436	0.3620	0.2711		210		
109.050	8.3	0.6632	0.5724	0.3907	0.2999	0.0274			
114.220	5.4	0.7051	0.6143	0.4326	0.3418	0.0693			
119.280	2.7	0.7445	0.6537	0.4721	0.3812	0.1087			

Here, LCQ=1083. From this we can identify:

- 00l type peaks. The first allowed peak is 002. From this, we can find C. Look for the value of $\sin^2\theta$ that increase by factors of 4, 9, 16... i.e. $l = 1, 2, 3, 4 \dots \lambda = 1.54062$
- the 4th peak as 102 because we observe the LCQ for $\sin^2\theta - 1A$. Recall that the 1 comes from the quadratic form of Miller indices (i.e. $h^2+hk+k^2=1$)
- the 8th peak as 112 because we observe the LCQ for $\sin^2\theta - 3A$. Recall that the 1 comes from the quadratic form of Miller indices (i.e. $h^2+hk+k^2=3$). We identify the 11th peak as...etc.

Peaks that are not either hk0 or 00l can be identified using the values of A and C in our formula. The allowed values are cycled and compared with $\sin^2\theta$ values.

Table 6: Lattice parameter of Titanium (sample-2) - a non-cubic Crystal by Analytical method.

Peak (2θ)	I/Io	Sin ² θ	hkl	Sin ² θ (calculated)
35.100	25.5	0.0909	100	0.0908
38.390	25.6	0.1081	002	0.1081
40.170	100	0.1179	101	0.1179
53.000	12.8	0.1991	102	0.1989
62.940	13.4	0.2725	110	0.2725
70.650	13	0.3343	103	0.3341
74.170	1.8	0.3636	200	0.3633
76.210	13.1	0.3808	112	0.3806
77.350	9.3	0.3905	201	0.3903
82.200	1.7	0.4321	004	0.4324
86.740	2.1	0.4716	202	0.4714
92.680	1.8	0.5234	104	0.5232
102.350	4.4	0.6069	203	0.6065
105.600	1.4	0.6345	210	0.6358
109.050	8.3	0.6632	211	0.6628
114.220	5.4	0.7051	114	0.7049
119.280	2.7	0.7445	212	0.7439

Once A and C are known, the lattice parameters can be calculated. $a=2.0951\text{au}$, $c=4.686\text{au}$ then, $c/a=1.588\text{au}$